Geologica Acta, Vol.13, Nº 2, June, 137-153
DOI: 10.1344/GeologicaActa2015.13.2.5

geologicaacta

Bedform variability and flow regime in a barrier-inlet system. The mesotidal Piedras mouth (Huelva, SW Spain)

J.A. MORALES[1] **I. DELGADO**[1] **J.M. GUTIÉRREZ MAS**[2]

[1] **Departamento de Geología, Universidad de Huelva**
Avda. 3 de marzo, s/n, 21007 Huelva, Spain

[2] **Departamento de Ciencias de la Tierra, Universidad de Cádiz**
Campus Río San Pedro, s/n, Puerto Real, Cádiz, Spain

ABSTRACT

Bedform fields from the Piedras River mouth (Huelva, SW Spain) have been studied using side-scan sonar techniques, combined with visual scuba-dives, and direct geometric measuring. The dominant flow regime has been determined from the results in these tidal environments, where erosive processes dominate during ebb, transporting sand as a bedload towards the mouth and central sector of the tidal channel. The process is reversed during tidal floods. During neap tides, larger bedforms maintain their geometry and position, whereas small ripples are re-oriented under different tidal conditions. Sand patches, dunes and ripples are interpreted as sediment bypassing zones. Large forms indicate high energy flow, which can only migrate when flow velocity reaches threshold values for the movement, with net sand transport towards open areas. Depositional features indicate low, moderate, and high-energy conditions. Here, a depositional regime dominated by sediment accommodation is dominant, where sandy sediments are continuously remobilized, transported and re-deposited, even closer to the estuarine mouth. In inner zones finer particles, such as clay and silt, are transported by tides as suspended matter and deposited in protected inner areas. The final results are long narrow tidal flats, which alternate with sandy areas dominated by erosion.

KEYWORDS **Estuary. Ebb-tidal delta. Bedforms. Flow regime. Sedimentary dynamics.**

INTRODUCTION

Subaqueous dunes are a frequent feature observed in estuarine environments (Dalrymple and Rhodes, 1995; Duck *et al*., 2001; Morales *et al*., 2006). The main part of the studied estuarine dunes are located in macrotidal systems. This kind of forms have been described by Langhorne (1973) in the Thames Estuary (UK), Knebel *et al*. (1992) in Boston (USA), Harris and Collins (1984) in the Bristol Channel (UK), Sherwood and Creager (1990) in the Columbia Estuary (USA), Garnaud *et al*. (2003) in the Seine mouth (France) and Van Lancker *et al*. (2004) in the Teignmouth Estuary (UK). Minor estuarine bedforms are also described in microtidal systems like those described by McKinney *et al*. (1974) in New Jersey (USA), and Woodruff *et al*. (2001) in the Hudson Estuary (USA). Although the works about subaqueous bedforms in mesotidal systems are relatively scarce, some few examples are well characterized. Examples of these mesotidal forms were described by Fenster *et al*. (1990) in Long Island (USA), Knebel *et al*. (1992) in Boston (USA), Cuadrado *et al*. (2003) in Bahía Blanca (Argentina) and Wu *et al*. (2009) in the Yangtze Estuary (China). The depositional features, essentially the different bedform fields, are generated by currents on the marine floor and the mechanisms of genesis can be established by means of their analysis (Ashley, 1990; Harbor, 1998; Carling *et al*., 2000). In estuarine mouths, the different bedform fields are generated by well defined

depositional mechanisms. In a general way, these are the result of the interaction of hydrodynamic agents, such as waves, tidal and fluvial currents (Davis and Kuhn, 1985; Nichol and Boyd, 1993; Costa *et al.*, 2009; Gutiérrez-Mas *et al.*, 2009a). In river mouths characterized by the absence of fluvial discharges and inlets, tidal currents are the main hydrodynamic agents involved in sediment exchange processes between the open sea and internal estuarine zones, exercising also a significant influence on adjacent shorelines (Fitzgerald, 1988; Hicks and Hume, 1996; Hicks *et al.*, 1999; Fitzgerald, *et al.*, 2002; Van Heteren *et al.*, 2006).

Flow regime of tidal inlets and estuaries is commonly deduced from the analysis of bedforms described by using side-scan sonar recordings. This technique was employed in the last decades to describe bedform fields, as well as dimensions and orientations of bedforms (McKinney *et al.*, 1974; Wright *et al.*, 1987; Kuijpers *et al.*, 1993; Anthony and Leth, 2002; Lobo *et al.*, 2004; Morales *et al.*, 2006; Gómez *et al.*, 2010; Gutiérrez-Mas *et al.*, 2009b). This paper studies seabed morphology inside of a shallow barrier-inlet system closing the Piedras River mouth with the aim to compare the dominant hydrodynamic regime deduced from the observed bedforms with the currents that act on their associated tidal sedimentary environments.

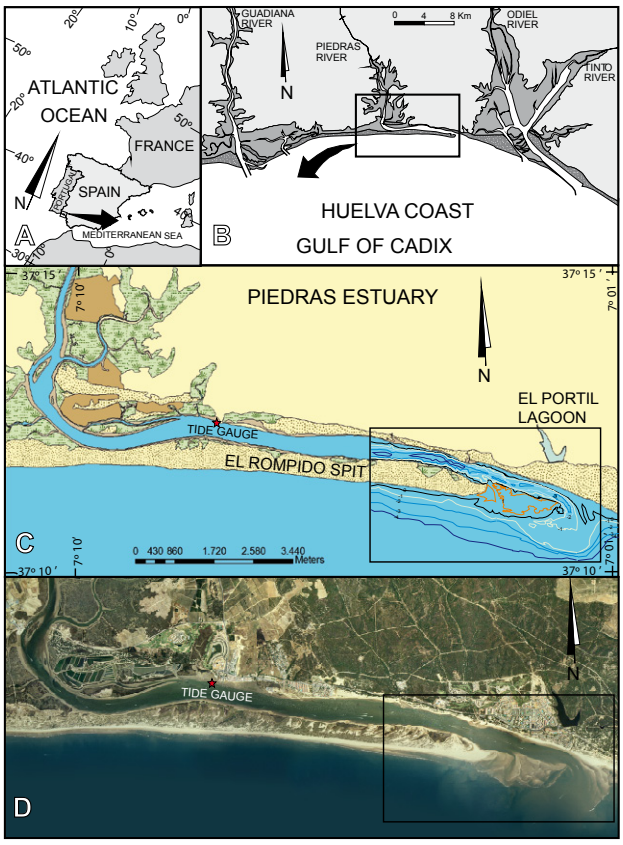

FIGURE 1. Location of the study area.

REGIONAL SETTING

The Piedras River mouth is located in the southwestern coast of Spain. The inner part of this estuary is characterized by its narrow shape and north-south orientation that is controlled by tectonic features of the Tertiary geological substrate. The closure system of this estuary (Fig. 1) is a long spit named El Rompido, which was built from some previous barrier islands and is undergoing apical growth of more than 30m/year from west-to-east (Ojeda and Vallejo, 1995). The apical growth is due to the attachment of sandy bars displaced by waves in the littoral drift sense. These two main orientations generated the characteristic L-shape of the whole estuarine channel. The frontal zone of this system is developing a classic ebb-tidal delta (after Oertel, 1972), which is also experiencing west-to-east migration as a result of a bar accretion process (Morales *et al.*, 2001).

This system is mesotidal semidiurnal, with a mean tidal range of 2m, oscillating between 2.82m during the spring tides and 1.22m during neap tides (Morales *et al.*, 2001). Fair weather waves dominantly come from the SW, with mean significant heights of 0.50m and mean periods of 4.03s. In addition, this coast is also affected by occasional SW or SE storms. A mean of 15 storms a year can affect this system, with mean significant height of 3.80m and extreme waves reaching 6m (Morales, 1997). The action of storms influenced the normal functioning of the ebb-delta system. Previous works described a cyclic model in the migration of the main ebb-channels (Morales *et al.*, 2001). The starting point of the first stage in this cyclical model is the opening of a new ebb-channel breaching the swash platform during a severe storm linked with a spring tide. Storms can also modify the position of the swash platforms and change punctually the dynamic of all the bedforms of the system.

Although geomorphological and sedimentological studies have been carried out in the Piedras River mouth (Dabrio, 1982; Borrego *et al.*, 1993; Ojeda and Vallejo, 1995; Morales *et al.*, 2001; Delgado *et al.*, 2005 and 2007), the dynamics of the tidal transport in the main channel and ebb-tidal deltas hadn't been studied yet.

METHODS

Subtidal and intertidal morphology was studied using side-scan sonar, with a C-MAX CM2000 with a frequency of 325kHz, and a range of 50m per band. Bedform field distribution was studied during two surveys carried out in February-March 2005 and October 2007. Fluvial discharge during surveys was less than 1m^3/sec, corresponding

with no rainfall. It must be taken into account that there is a hydrologic dam located right at the last point of tidal influence. Navigation was done in parallel lines so that successive navigation lines superposed 20% of that recorded. Accuracy of the sonographic recording position was confirmed by sonar connected to a Garmin e-Trex Vista GPS and to a laptop computer using Ozi-Explorer GPS software.

Tidal levels were determined by means of a tide gauge located in the inner estuary (Fig. 1). Stream speed was measured using a Silva Sea Data current-meter, which has a minimum accuracy of 0.003m/s. Current velocities were obtained 70cm above the bed to study the water-sediment interface. Data were measured during different tidal ranges, which were carried out on: February 18th, 2005 (neap tide, 0.97m of tidal range); March 11th (spring tide, 3.42m of tidal range) and March 21st, 2005 (mean tide, 1.41m of tidal range).

In order to accurate similar tidal current regimes, side-scan sonar surveys were carried out during three tides of similar ranges to those in which the currents were measured: 11th of February, 2005, (spring tide, tidal range of 3.23m); 21st of February, 2005 (mean tide, tidal range of 1.82m) and 18th of March, 2005 (neap tide tidal range of 0.91m). Sonographic mosaics were geo-referenced and created using ArcGIS 9.1. Subtidal bedform analysis was performed using sonagraphic recordings taken with MaxView software (official software by C-Max Ltd.), which includes an application for measuring distances and heights. Geometrical dimensions of bedforms were checked by performing scuba-dives and taking direct pictures and videos. In the intertidal zone, bedforms were directly measured during low tides. A millimetrically graduated 20m long reel was used to measure distance between ridges. The height of minor forms was measured using a plastic caliper. Bedform ridge orientation was measured with a Silva compass. To classify bedforms, according to criteria from Ashley (1990), the relationship between bedform heights (H) and distance between ridges (L) was used. In addition, 15 samples of sediment were taken in different subenvironments using a van been type drag. Grain size analysis of these samples were developed by means of a laser difractometer Malvern Mastersizer 2000M in dry way.

RESULTS

Geomorphology and Sedimentology

The sub-environments of this estuarine mouth were previously described by Morales *et al*. (2001), These are similar to those described elsewhere (*e.g*. Oertel, 1972; Hayes, 1980; Imperato *et al*., 1988; Sha, 1990) and maintain a constant relationship with the tidal levels, the magnitude of flood and ebb currents and the degree of influence of waves. Nevertheless, for this work different hydrodynamic zones have been distinguished from a physiographic and depositional point of view (Fig. 2). The sediment variability is not very high along this system. From a sedimentological point of view, the records of side-scan sonar and sediment sampling contributed to elaborate a cartography of the different lithologies present in the beds of the studied channels (Fig. 3). The medium sand is the dominant fraction with small amounts of coarse and fine sand. All the analyzed samples can be classified in four grain-size distribution classes (P1 to P4) that correspond with different sub-environments (Fig. 2).

Estuarine channel

It corresponds to areas protected from waves by the littoral spit. From a morphodynamic point of view, two different areas can be distinguished in this environment: deep and shallow areas. The areas deeper than 2m below the Extreme Equinox Low Water (EELW) level are zones of well-sorted medium and fine sand (Class P3 in Fig. 2). The maximum depth in this area is 4.5m under the EELW. Previous works interpreted them as zones of sediment bypass, whose position changes from one bank to another, similarly to what occurs in a straight river (Morales *et al*., 2001). The most common bedforms are ripples and small and medium dunes.

In the shallow area, three types of substrates, sandy, muddy and rocky are recognized. Outer shallow margins are characterized by sandy beds. The bed in the innermost estuarine margin is usually muddy, showing erosive and anthropogenic marks such as anchor and network traces (A). The most common shallow areas especially on the backside of the spit, are rocky shoals (Fig. 4B).

Main ebb channel

It represents the continuity of the estuarine channel through the ebb-tidal delta system connecting it with the open sea. The bed is also made of well sorted medium-fine sand (Class P3 in Fig. 2). This sandy bed is covered by abundant ebb-oriented transverse bedforms, whose crests are perpendicular to the tidal channel axis (Fig. 4C and D).

Marginal flood channel

Medium sand beds with coarser sediment than in the main ebb channel because it includes coarse-very coarse sand and gravel, mainly composed of shell fragments (Class P1 in Fig. 2). Flood-oriented small bedforms are dominant, showing crests perpendicular to the channel axis (Fig. 4E).

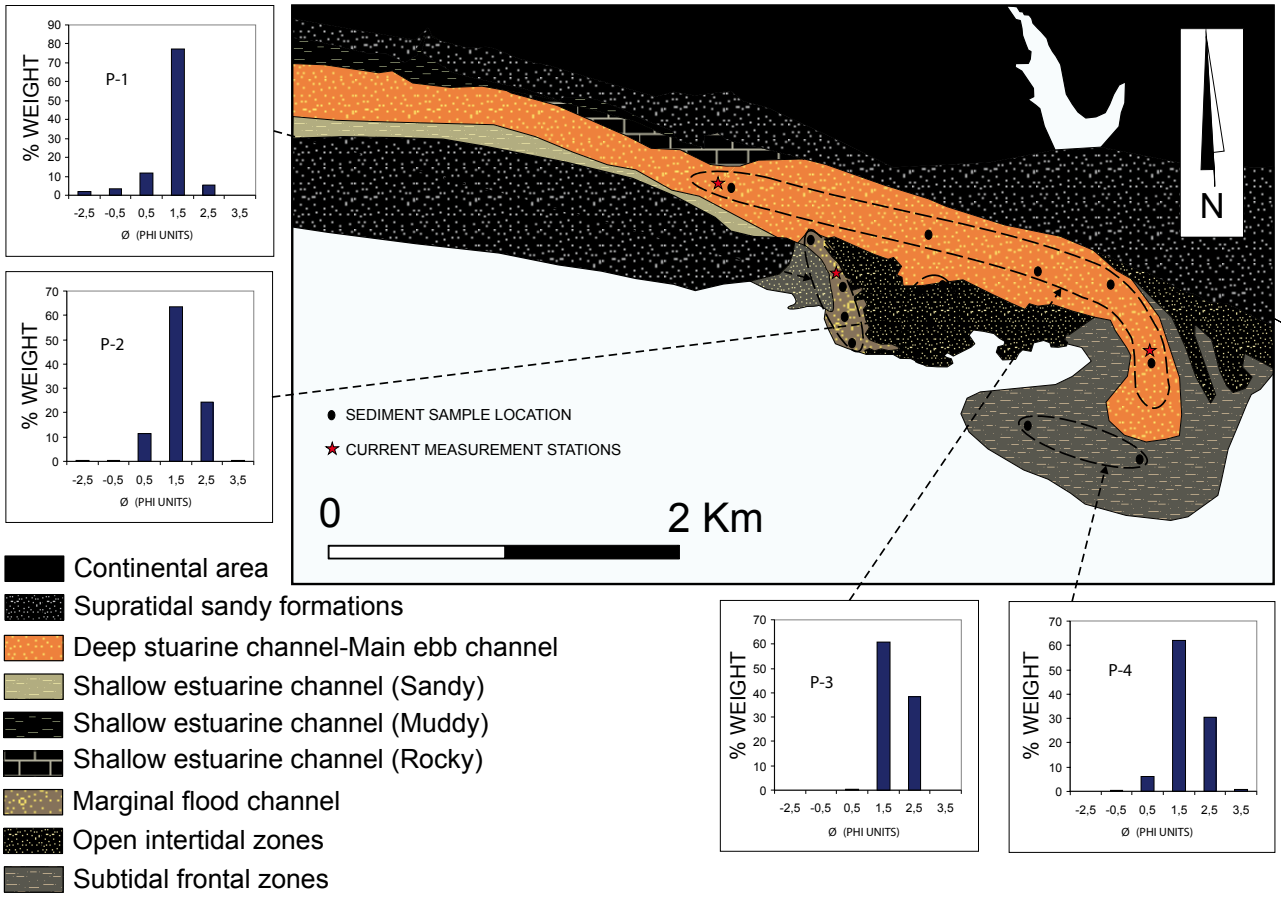

FIGURE 2. Environments and sediment distribution on the estuarine bed with histograms of the four main types of sediment after their grain size distribution (P1 to P-4). P1: well sorted medium sand (marginal flood channel). P2: very well sorted medium sand (open intertidal zones). P3: moderately sorted medium-fine sand (estuarine and main ebb-channels). P4: well sorted medium-fine sand (subtidal frontal zones).

A parabolic flood-oriented macroform, with superimposed medium dunes, is developed whese this environment and the estuarine channel converge.

Open intertidal zones (ebb-tidal delta levees)

They are located in open marine areas, exposed to wave action and consist of long sandy levees, which act as swash platforms that form wave bars. The dominant sediment consists of medium sand, with minor fractions of coarse and fine sand (Class P2 in Fig. 2). Straight-crested bars are usually located in front of levees and migrate landwards by wave action. Smaller tidal and wave bedforms are developed on the bars.

Subtidal frontal zones (front delta lobes)

They are located under the mean low water level just in front of the main ebb channel mouth. The bed on the lobe is made of medium fine sand (Class P4 in Fig. 2). The total absence of very coarse sand and gravel and a low coarse/fine ratio marks the difference with the Class P2.The western part displays erosive features, such as those that can be observed in older sandy formations. These areas are heavily reworked by human activity, showing abundant trawling marks right in front of the main ebb channel (Fig. 4F).

Hydrodynamics

As expected, the curves of current velocity show remarkable differences between tides of different range, but current velocity differences can also be observed by comparing the curves of the same tide in the different channels (Fig. 5).

Neap tides

During the flood of neap tides, weak currents are developed in the estuarine channel (9.90cm/s) and in the main ebb channel (21.08cm/s). At the same time, the flood in the marginal flood channel reached 27.12cm/s. On the contrary, during the ebb cycle, the strongest currents have

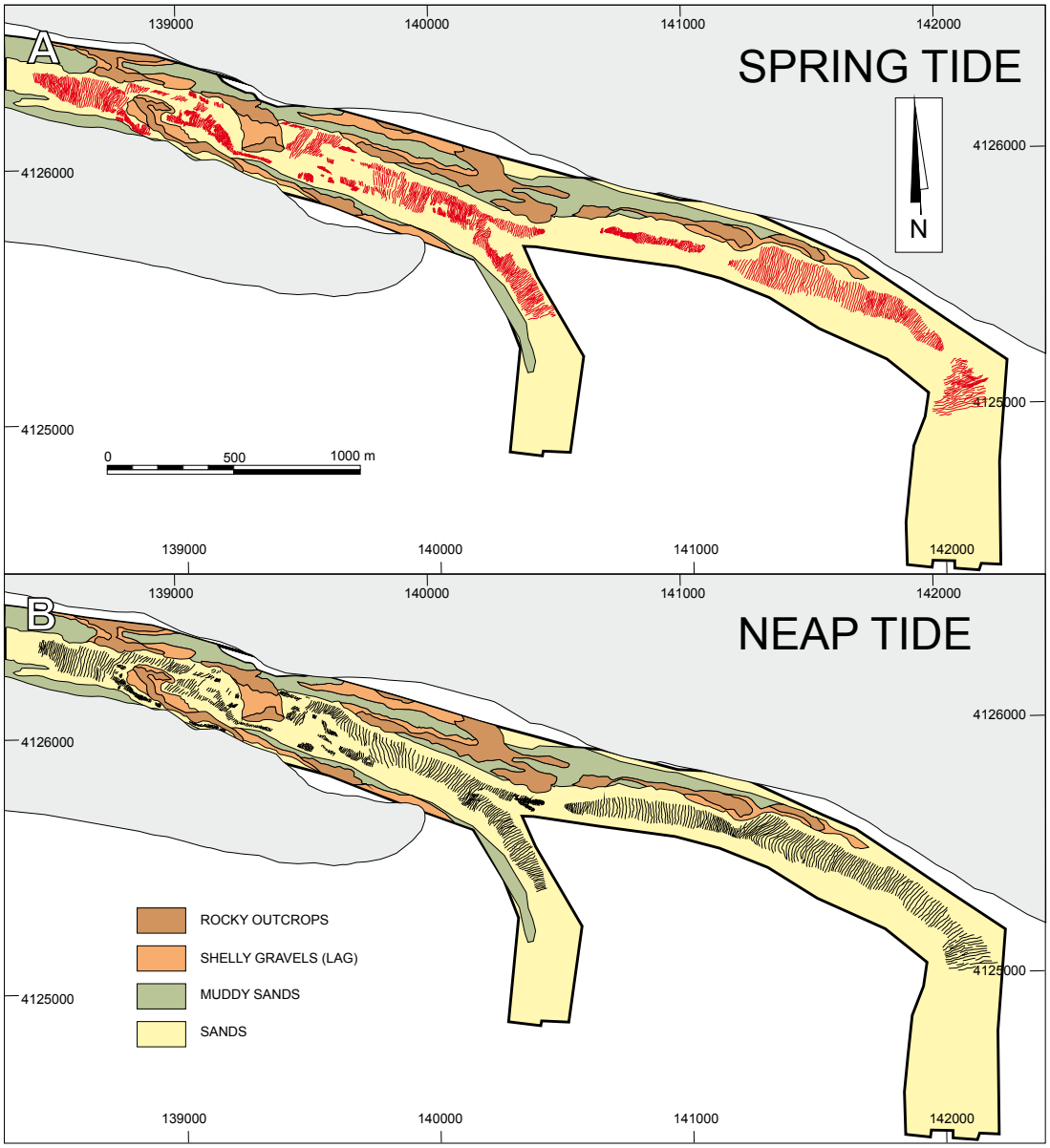

FIGURE 3. Maps of bed distribution based on mosaics of Side-scan sonar. A) Spring tides. B) Neap tides.

been measured just in the estuarine channel (47.10cm/s), whereas in the main ebb channel and the marginal flood channel current velocities wese similar (32.85 and 28.72cm/s respectively).

Mean tides

In contrast with the neap tides, during the flood of mean tides the strongest currents of the system wese observed in the estuarine channel (49.85cm/s). Currents of similar velocity were measured in the marginal flood channel (49.70cm/s), whereas in the main ebb channel currents were a little slower (38.80cm/s). During the ebb cycle, currents in the three channels reached similar velocities. In the estuarine channel 51.75cm/s, in the main ebb channel 52.80cm/s and in the marginal flood channel 47.06cm/s. In all cases, a great asymmetry is observed in the current velocity curves, but whereas in the estuarine channel and main ebb channel is the ebb the dominant current (in velocity and duration) in the marginal flood channel the flood is 1h 30' longer than the ebb.

Spring tides

In the case of the spring tides the estuarine channel presents a curve clearly symmetric respect to the duration of the cycles, but not respect to the velocity current velocity (56.10cm/s during the flood and 70.05cm/s

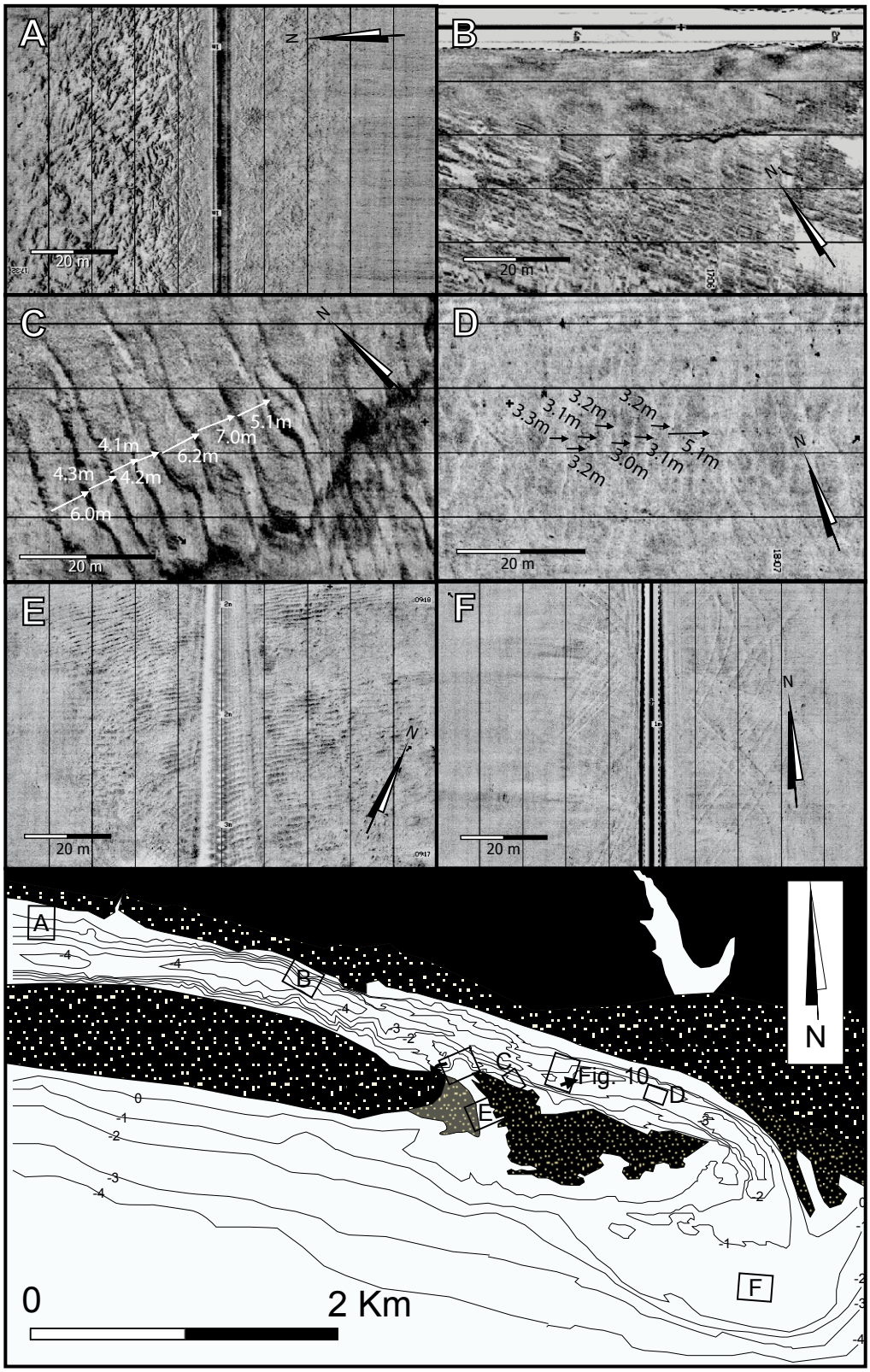

FIGURE 4. Side-scan sonar records with indication of their position in a bathymetric map of the studied area. A) Muddy bed with erosional features (right) and sandy plane bed (left). B) Rocky bed. C) Medium dunes with sinuous crests oblique to the channel margin. D) Medium dunes with straight crests. E) Small dune fields on the marginal flood channel. F) Plane bed on the ebb delta lobe with marks of fishing activities.

during the ebb). The curves obtained in the main ebb and marginal flood channels are completely asymmetric. The spring flood in the main ebb channel displays a velocity peak of 57.90cm/s, but the ebb has longer duration and reaches 82.70cm/s, being the dominant current in this channel. On the contrary, in the marginal flood channel is the flood the dominant current, reaching 78.12cm/s versus the 65.87cm/s reached during the ebb. In this case, both cycles have a similar duration of 6h 10'.

Bedform morphology and dimensions

Mesurements of bedform dimension parameters (wave height and length) were performed along the previously described environments.

Estuarine channel

The estuarine channel shows a great diversity of bedforms, as well as a high bedform variability over time (Table 1). When channel margin is muddy or rocky, bedforms are absent (Fig. 6A and B). Large sand patches typically appear on around submarine rocky outcrops. During spring tide conditions, the main bedforms observed are: medium dunes with straight crests (2D dunes) or sinuous crests (3D dunes) (Fig. 6C and D). Lateral large dunes turn into straight or linguoid small dunes. These bedforms are superimposed by smaller straight, sinuous or linguoid ripples (Fig. 6E and F). Bedforms formed during mean tide conditions show great diversity. In the middle of the channel, straight to linguoid medium 2D or 3D dunes appear (Fig 4A). Small 2D dunes are present along the shore of the channel. Small straight and linguoid ripples are superimposed on large bedforms. During neap tide conditions, large bedforms show similar dimensions to those observed during mean tides, although they are smaller in size, with straight ripples on the stoss side. Large bedforms are formed in the direction of the ebb and develop ridges with N50°E to N30°W directions, crosswise to the channel axis (Fig 4B).

Main ebb channel

The main ebb channel displays abundant bedforms of different morphology and size according to tidal ranges (Table 2). During spring tide conditions straight small 2D dunes appear, superimposed on them with smaller linguoid ripples. During mean and neap tide conditions, small 2D dunes are also observed. Bedforms are always formed in the direction of the ebb. Their crests have N12°E to N170°E directions and form angles of 20 to 35° with the channel axis (Fig. 4C). The only bedforms formed in the direction of the tidal flood are linguoid ripples developed during spring tides.

Marginal flood channels

During spring tide conditions, sinuous medium dunes 3D dunes developed in both flood and ebb tides (Table 3, Fig. 4D, 7A and B). The larger bedforms have a distance between crests from 5.0 to 5.3m. During ebb, large bedforms show similar dimensions and sinuous ripples superimposed on them (Fig. 4E). Crests are oriented from N90°E to N105°E, almost perpendicular to the channel axis. Mean tide conditions are characterized by the presence of straight small dunes 2D dunes oriented in the direction of the tidal flood, with crests perpendicular to the channel axis (N84°E).

TABLE 1. Main geometric and depositional features of the bedforms observed in the estuarine channel of the Piedras River mouth

Bedform	Bedform geometry			Flow			Energy
	Dimensions (m)	Crest morphology	Crest orientation	Tidal flow	Tidal range	Max. Flow speed (m/s)	
Medium dunes	L= 5.00–8.30 H= 0.40–0.80	Straight Sinuous	N20–10ºW	Ebb	Spring tide	0.70	Medium–High
Small dunes	L= 2.30–5.00 H= 0.20–0.50	Straight linguoid	N20–10ºW				Medium
Ripples	L= 0.40–0.50 H= 0.32–0.40	Straight linguoid	N20–10ºW				Low
Medium dune	L= 5.50–9.80 H= 0.40–0.85	Straight linguoid	N45–30ºW		Mean tide	0.52	Medium–High
Small dunes	L= 2.50–4.00 H= 0.25–0.50	Straigh	N30–50ºE				Medium
Ripples	L= 0.50–0.60 H= 0.38–0.45	Straight linguoid	N30–50ºE				Low
Medium dunes	L= 5.40–9.30 H= 0.38–0.79	Straight linguoid	N30–50ºE		Neap tide	0.47	Medium–High
Small dunes	L= 1.50–4.70 H= 0.10–0.30	Straight linguoid	N30–50ºE				Medium
Ripples	L= 0.45–0.50 H= 0.03–0.04	Straight	N30–50ºE				Low

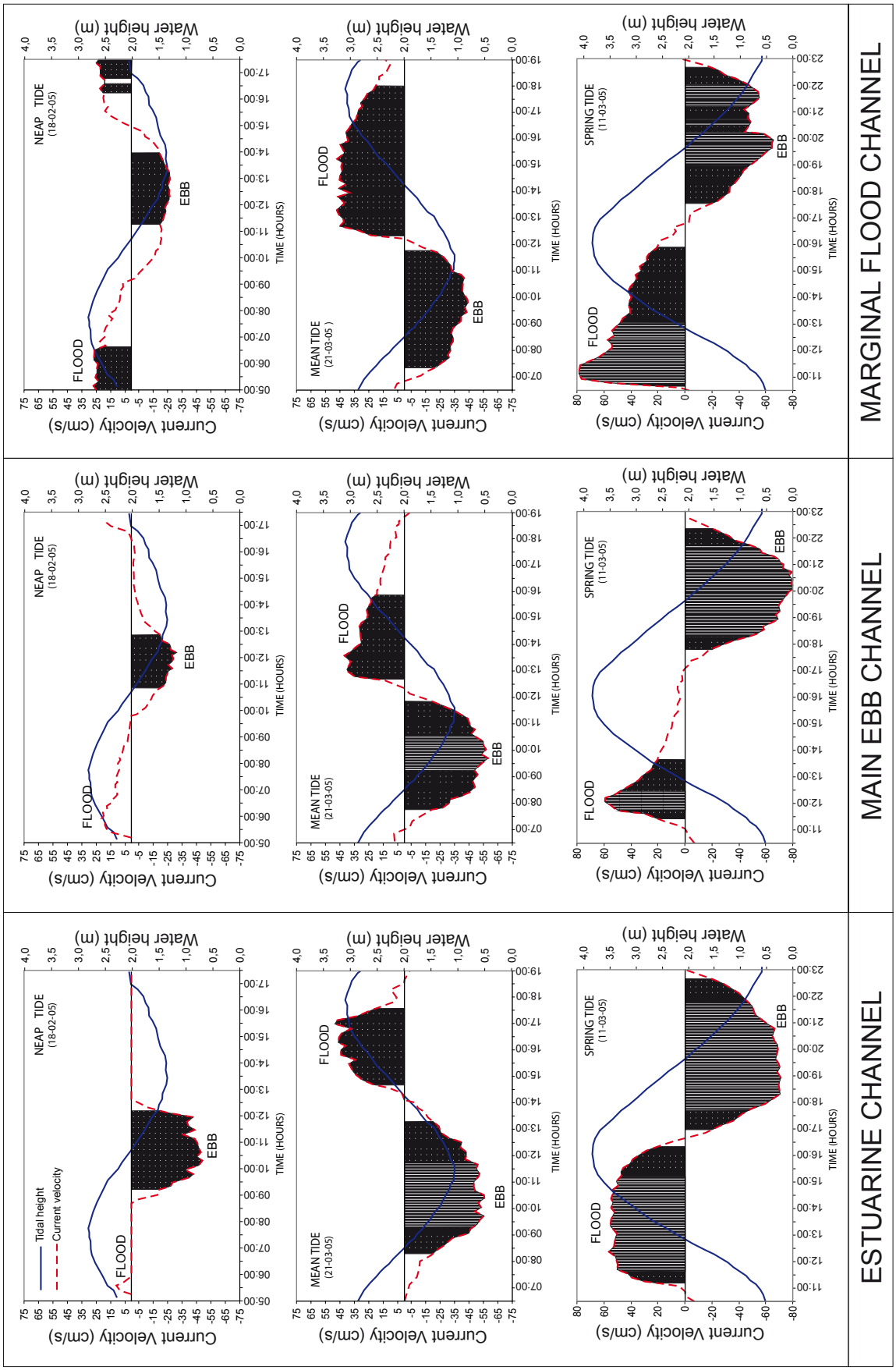

FIGURE 5. Current velocity curves indicating bedform movement thresholds. Points indicate the ripple field stability. Vertical stripes indicate the dune field stability.

Open intertidal zones (ebb-tidal delta levees)

They are located on the open side of the barrier-island, and are thus affected by waves and tidal action (Table IV). During spring tide conditions, a wide range of bedforms are observed. In the inner zones medium linguoid dunes are observed (Fig. 7C and D), with linguoid ripples superimposed on them. In the middle of the swash platform large sinuous bedforms appear. Sinuous ripples with forked crests are formed in runnels perpendicular to larger bedform crests (Fig. 7E). In most open zones, small linguoid dunes are observed, whith smaller bedforms, such as linguoid ripples superimposed (Fig. 7F). As all the measurements were done in low tide, the bedforms were oriented in the sense of the ebb migration, with directions close to N12°E. In the middle of the platform, the directions of bedforms range from N30°E to N65°E, while the outermost bedforms show crests in a N82°E direction (Fig. 8).

During neap tide conditions, bedform variability is smaller, and mostly associated with sea swells. Elongated sandy banks or straight-crested wave bars are observed. These bars tend to be situated in front of levees and migrate towards land due to sea swell. Small 2D dunes and symmetrical straight ripples are formed on these bars, which both show small dimensions and are short-lived (Fig. 7G and H). 2D dunes and ripples present orientations close to N90°E, parallel to the coastline.

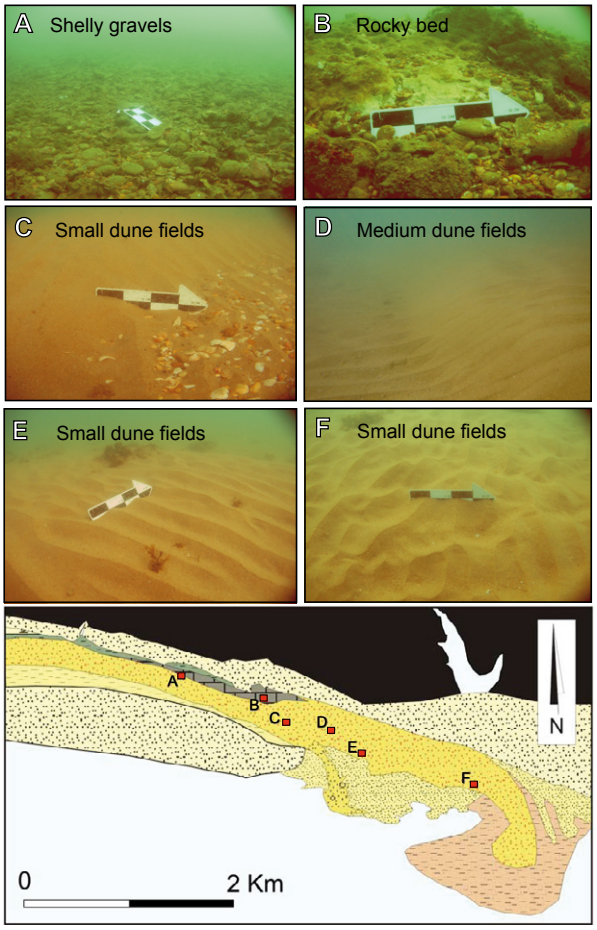

FIGURE 6. Underwater photographs of bed, with indication of their position in the map. A) Lag of shelly gravels. B) Erosive rocky bed. C) Small dunes with superimposed ripples. D) Medium dunes with superimposed interference wave ripples. E) Straight crested ripples. F) Linguoid ripples. The length of the arrow used as scale is 20cm, black-and-withe subdivisions are 5cm long.

INTERPRETATION

Bedform dynamics

From a hydrodynamic point of view, tidal currents constitute a primary agent of transportation. Sandy lithologies are a highly mobile. Sand is transported as bedload from fluvial zones towards the open sea and tidal currents act as an effective bypassing mechanism that leads a great amount of eroded sand from the island bar, to later be transported along the channel to the sea. From the orientation of dominant bedforms it is deduced that the estuarine and the main ebb channels are predominantly dominated by ebb currents. The major ebb-oriented forms eventually remain in the same orientation because the flood current has not enough velocity to reverse the major bedforms. Nevertheless, the flood is able to develop minor bedforms that migrate landwards and to reshape the crest of the major forms. Marginal flood channels develop bedforms that are oriented landwards because flood currents are dominant in these environments. Open intertidal areas show sand movement landwards as waves move sand as straight-crested wave bars in this direction. These deductions from direct observation of dune fields, can be corroborated by analysing the tidal current velocity through time (Fig. 5).

In the intertidal areas, all bedforms observed are ebb-oriented, with a rotation of the main direction of crests due to the deviation of the current by the topography. In these areas, there is a notable influence of the flow depth that varies with time. The maximum depth is about one meter and this induces an increasing of the shear stress on the bed, producing more energetic forms according with the arguments of Rubin (1987). Subtidal frontal areas (ebb-delta lobes) show evidence of lateral migration due to the combined action of ebb and waves, which act in opposite directions producing an area of hydrodynamic shadow. In any case, the presence of erosive features on the western face of the lobes is an evidence of eastward migration.

An analysis of the bedform dynamics may be done by representing the thresholds for bedforms stability fields deduced from the diagram suggested by Harms *et al.*

TABLE 2. Main geometric and depositional features of the bedforms observed in the main ebb channel of the Piedras River mouth

Bedform	Bedform geometry			Flow			Energy
	Dimensions (m)	Crest morphology	Crest orientation	Tidal flow	Tidal range	Max. Flow speed (m/s)	
Small dunes	L= 3.50–3.30 H= 0.40–0.60	Straight	N12–170ºE	Ebb	Spring tide	0.84	Medium
Ripples	L= 0.30–0.35 H= 0.04–0.06	Linguoid	N12–170ºE	Ebb-Flood		0.58	Low
Small dunes	L= 1.60–2.70 H= 0.30–0.50	Straight	N12–170ºE	Ebb	Mean tide	0.60	Medium
Small dunes	L= 0.65–0.70 H= 0.60–0.70	Straight	N12–170ºE				Medium

(1975) on the current velocity curves measured in different sedimentary sub-environments during different tidal cycles (Fig. 5 and 9). The bedform behave as follows.

During neap tide conditions, flood currents fall under the limit for ripple formation, while ebb currents only reach the threshold for straight ripples to be formed as tidal flow does not act long enough to transform them into linguoid ripples. These data confirm that the largest bedforms observed during neap tide conditions are inherited forms, generated during a previous stage, when currents were stronger than those found during neap tide conditions. Large bedforms present during neap tide conditions are of similar dimensions, or even higher, than those observed during spring and mean tides, which indicates that neap tidal currents are incapable of changing forms produced during mean tide conditions, although they can modify their crests, causing them to lose height.

During mean tide conditions, both flood and ebb currents reach the threshold for ripple and 2D dune formation, with linguoid ripples as the most stable bedform. A coarser grain size observed in secondary channels would explain the existence of larger bedforms, which would be stable at lower velocities. Both ripples and dune are balanced with respect to tidal current velocity. The largest dunes, such as those that form during neap tide conditions, are inherited bedforms, generated during previous spring tide current situations.

During spring tide conditions, the current velocity reaches the limit for dunes formation, in both flood and ebb situations. Ebb bedforms are the most abundant because these forms remain stable longer than flood bedforms, the reason they are the most abundant bedforms could be explained. Flood bedforms are more stable at upper topographic heights than ebb forms, which would explain the reverse bedforms that are observed. It should be pointed out that the bedforms observed, during both flood and ebb, are in concordance with velocities developed by currents during tidal cycles, and can therefore be interpreted as being active forms.

On the other hand, dominance of mesoform asymmetry during ebb and symmetry during flood, together with maintenance of length between crests, suggest an inability of floods to invert the form migration direction. Flood action is just reflected in crest reshaping, which will ultimately mean the development of a reactivation surface. This interpretation also tallies with velocity data for currents measured during the campaign, which revealed up lower values for flood currents (Fig. 5). When the current reverses, only smaller bedforms show significant changes of morphology and orientation. It can be observed that ebb-oriented forms are

TABLE 3. Main geometric and depositional features of the bedforms observed in the marginal flood channel of the Piedras River mouth

Bedform	Bedform geometry			Flow			Energy
	Dimensions (m)	Crest morphology	Crest orientation	Tidal flow	Tidal range	Max. Flow speed (m/s)	
Medium dune	L= 5.00–5.30 H= 0.25–0.30	Sinuous	N90–105ºE	Flood	Spring tide	0.91	Medium–High
Ripples	L= 0.25–0.40 H= 0.25–0.30	Linguoid	N90–105ºE	Ebb-Flood		0.66	Low
Small dunes	L= 0.90–1.90 H= 0.15–0.30	Straight	N84E	Flood	Mean tide	0.50	Medium

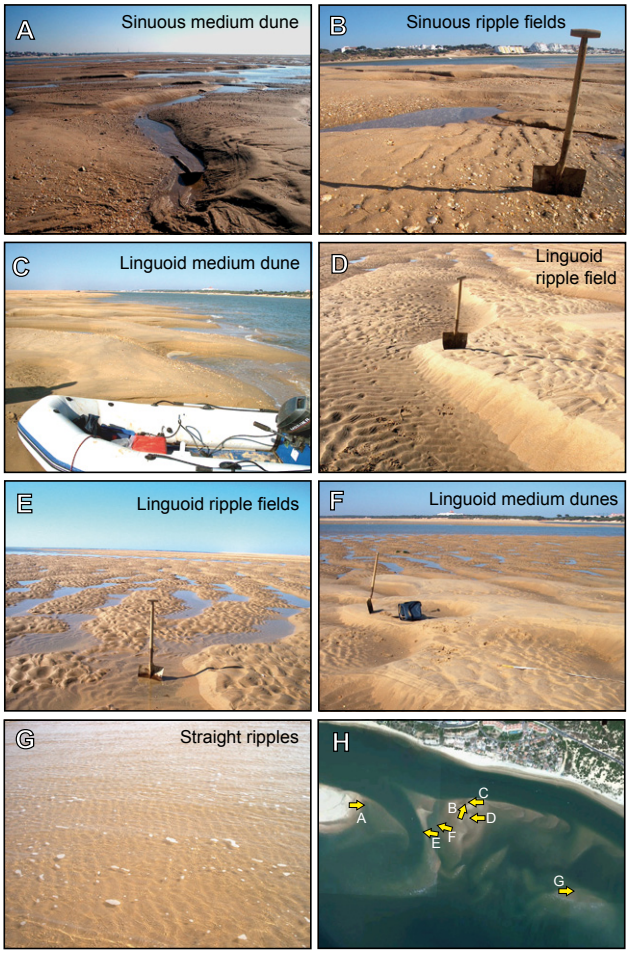

FIGURE 7. Dune fields located on intertidal zones. A) Medium straight crested dunes with reverse asymmetries in the margin of the marginal flood channel. B) Ebb-oriented sinuous ripple fields on the levee surface. C) Medium linguoid dunes located on the inner border of the levee. D) Sinuous dune field with superimposed linguoid ripples (ebb-oriented). E) Linguoid ripples reworking a small sinuous dune field. F) Medium linguoid dune field. G) Symmetric straight crested ripples. H) Location of the pictures with indication of the sense of view.

clearly asymmetrical, showing a seaward displacement (Fig. 10A). During flood conditions, medium and small dunes do not present a marked asymmetry. They present rounded crests in comparison with those produced during ebb (Fig. 10B). On the contrary, medium dunes maintain their dimensions, such as length between crests, which remain invariable although velocities during flood are of minor entity. The majority of these forms present an asymmetry in the ebb direction during both ebb and flood conditions. Dominance of asymmetric dunes during ebb and symmetric forms during flood, together with the maintenance of length between crests, suggest a dominance of the ebb current, so as an inability of floods to invert form migration direction. Flood action is only reflected in the reshaping of crests, which will eventually lead to the development of a reactivation surface. This interpretation also coincides with velocity data for currents measured during our campaign, which presented in all cases lower values for flow currents (Fig. 5). The only form with landward asymmetry is the parabolic macroform previously described in the chapter 3.1.3. (Fig. 10C and D). This form is located behind the mouth of the marginal flood channel and presents its maximum asymmetry during flood periods as well as medium dunes developed on its surface (Fig. 10D).

Flow and depositional regimes

Previous data indicate that dominant flow regime for the whole area is between low and medium, with maximum tidal flow velocities oscillating between 35 (neap) and 80cm/s (spring). Namely, the study zone showed a moderate level of hydrodynamism. However, a higher flow regime is observed in zones, such as ebb tidal delta levees. The only macroform observed, with dimensions of hundreds of metres in lenght, is interpreted as an equivalent of a flood spillover lobe, not reaching the category of flood-tidal delta because of a lack of space and dominance of ebb currents that impede the development of a flood ramp like in an intertidal zone. However, the system is able to develop a submerged ramp (Fig. 10C and D).

Bedform field distribution in the Piedras River mouth reveals a very mobile sea bed where sand is transported as a

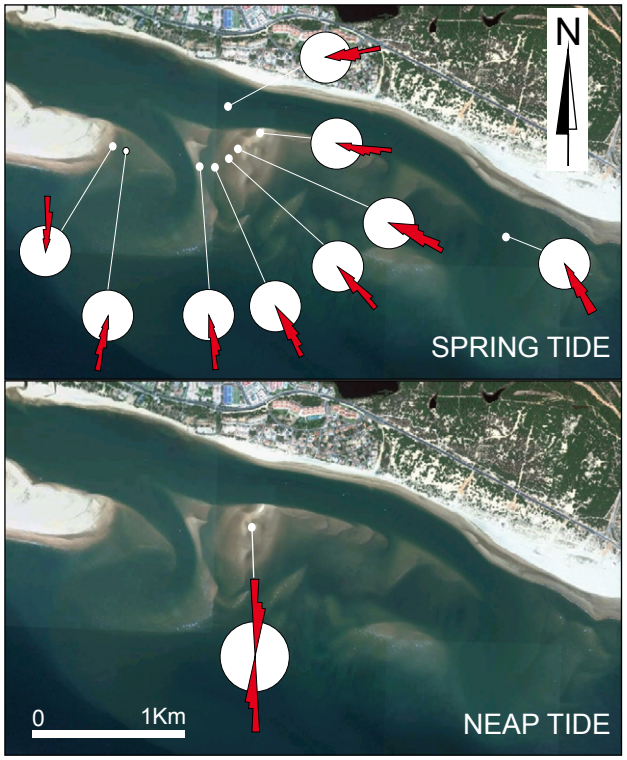

FIGURE 8. Rose-diagrams indicating the orientation and sense of migration of bedforms measured on the intertidal levees. Scale of arrows in rose-diagrams are proportional to the number of measurements per direction.

TABLE 4. Main geometric and depositional features of the bedforms observed in the main ebb-tidal delta levees of the Piedras River mouth

	Bedform	Bedform geometry			Flow			Energy
		Dimensions (m)	Crest morphology	Crest orientation	Tidal flow	Tidal range	Max. Flow speed (m/s)	
Back	Medium dunes	L= 4.90–7.65 H= 0.30–0.47	Linguoid	N12ºE	Ebb	Spring tide	0.84	Medium–High
	Ripples	L=0.17–0.25 H= 0.23–0.25	Linguoid	N12ºE			0.52	Low
Centre	Medium dune	L= 2.60–4.90 H= 0.18–0.24	Sinuous	N30–65ºE			0.66	Medium–High
	Ripples	L= 0.46–0.13 H = 0.07–0.16	Sinuous bifurcate	N120–155ºE			0.47	Low
Front	Medium dune	L= 2.10–2.58 H= 0.13–0.23	Linguoid	N82ºE			0.41	Medium–High
	Ripples	L= 0.54–0.24 H= 0.11–0.30	Linguoid	N82ºE			0.29	Low
Back	Large dunes	L= 10.00 H= 0.30	Straight	N90ºE	Ebb	Neap tide	0.29	High
	Small dunes	L= 1.20–1.25 H= 0.50–0.10	Straight	N90ºE				Medium

bedload along the deepest parts of the channels, generating different bedform fields, which are a depositional expression of the factors involved, mainly tidal flows and the quantity and quality of available sediments. On the contrary, in shallow marginal zones located in the innermost zones, the presence of muddy deposits indicates calm conditions and the deposition of fine particles from suspension.

In outside areas of the intertidal levees, bedform fields show a constant sand flow towards the zone of the estuarine channel. The direction of sediment transport changes during each tidal cycle and thus sand is subjected to an intensive process of progressive selection and re-working, as shown by sediment analyses. These data together with the presence of submarine rocky outcrops indicate a low rate of terrigenous and bioclastic sediment supply, as well as a depositional regime controlled by accommodation, although current velocities are not very high. Although there are sectors that support a high flow regime in the study area, such as ebb tidal delta levees, in general, the zone shows a moderate flow regime, which partly explains the stability and sustainability of this depositional environment and the permanence of a barrier island system developed at the Piedras mouth, despite low fluvial supply rates. Tidal currents are strong enough to erode the sea floor and maintain the depth of the channels while maintaining a depositional balance, such that the erosive-depositional effects for both flood and ebb are practically compensated.

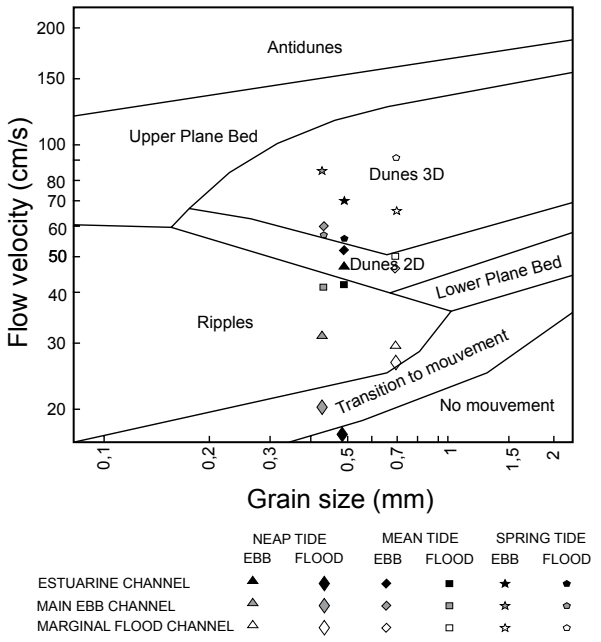

FIGURE 9. Bedform stability conditions for the medium sand under the maximum ebb and flood currents of the studied tides represented in the diagram of Harms *et al.* (1975).

While in tidal channels and inner zones tidal currents maintain a depositional balance, in open sea zones, successive wave trains act as a true energetic barrier that prevents sediments from escaping the littoral system. This regime is the dominant except during very high energy processes, such as major storms or tsunami waves that are able to generate a flow that is strong enough to destroy the barrier and transport sediments seaward (Morales *et al.*, 2008 and 2011).

DISCUSSION

Presence of sandy bedforms in tidal estuarine mouths is characterized by the interaction of stream speed, water

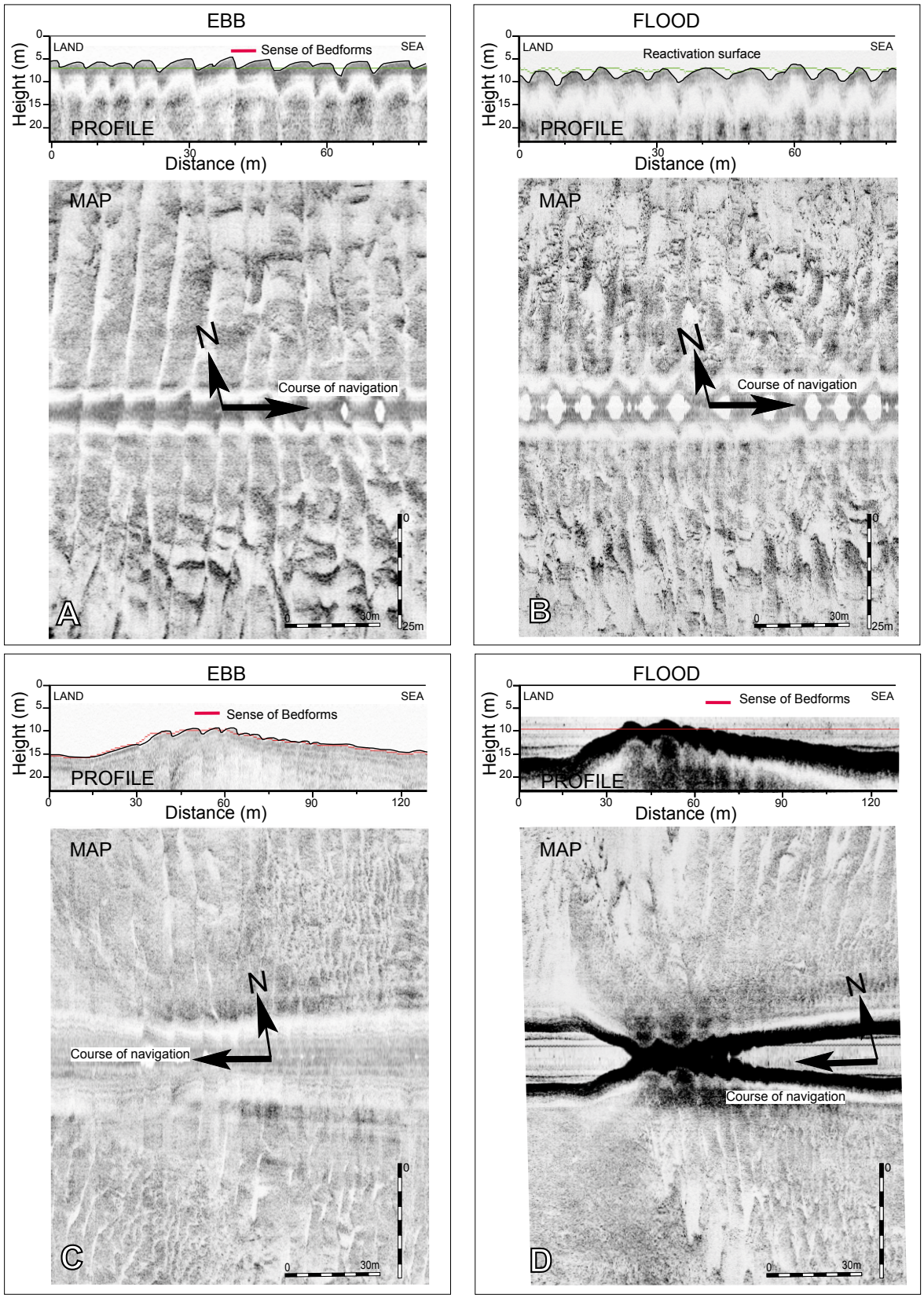

FIGURE 10. Bedforms under reverse flood conditions. A) Medium dune field under spring ebb conditions. B) The same dune field under spring flood conditions. C) Large dune with superimposed small dunes under spring ebb conditions. D) The same dune under spring flood conditions. (This large dune is located at the inner part of the marginal flood channel.)

depth, sediment grain size, sediment availability and flow regime. Understanding these interactions is fundamental to explain bedform field distribution, especially in the case of mesoforms as dunes (Aliotta and Perillo, 1987; Dalrymple and Rhodes, 1995; Cuadrado *et al.*, 2003). Bedform distribution in the Piedras estuarine mouth is the result of a combination of these factors. Dynamics of small bedforms such as ripples and small dunes are not of great interest as they reverse with the acting flow and are always in a dynamic equilibrium with it. On the contrary, the distribution, dimensions and shapes of larger dunes can explain particular aspects of flow dynamics, since these forms are often in a dynamic imbalance with acting currents but are good markers of dominant flow conditions (Fenster *et al.*, 1990) and hydrodynamic regimes (Grant and Madsen, 1982; Van Rijn, 1993).

In our case, both minor form and mesoform fields are composed of medium sand with minor percentages of coarse and fine sand and were developed in shallow areas where de deepest part of the channel reaches 4.5m. A short variability of mean grain size cannot confirm the fact suggested by Dalrymple and Rhodes (1995) and Bartholdy *et al.* (2002), who indicated that dune height progressively decreases as grain size becomes finer, or the correlation between grain size and height suggested by Southard and Boguchwal (1990). The height and wavelength of the dune fields studied here vary according to flow conditions without any observed variation of grain size. In addition, smaller dunes and ripples are observed towards the border of the field, normally near rocky outcrops (Fig. 3). This fact does not support observations made by Salsman *et al.* (1966) who found that dune height increases with a decrease in water depth. However, it does coincide with observations made by Dalrymple and Rhodes (1995), who indicated that dune height typically becomes smaller at the edges of dune fields where they move outwards into rippled sand flats. A possible explanation of our case could be in relation with an increase of bottom roughness on rocky shoals located in shallow margins, which could increase the shear stress and diminish the current velocity in water-bed interface on shoal borders. It is also possible, as it was well documented by Aliotta and Perillo (1987), that the presence of only small amounts of mobile sand over a hard substrate may inhibit the formation of dunes.

In shallower areas, and especially in intertidal levees, water depth seems to induce a control on dune dimensions and shapes. It is well studied that the combination of stream speed with flow depth and sediment size exerts a great control on bedform development (Rubin, 1987). In intertidal levees of ebb-tidal deltas, flow velocity and water depth are compensated during mean and spring tides, increasing the time of dune migration. When current velocity and depth decreases under the dune stability threshold, dunes stop their migration, and small ripples thus develop superimposing them.

Presence of dunes with superimposed smaller bedforms and dunes with dimensions, shapes and orientations that clearly show an unbalance with currents acting during the measurements is proof of the unsteady conditions of variables that control the development and morphology of the bedform. Normally, in order to develop equilibrium forms the system needs currents to be stable during enough time to reach a balance. This is called the "equilibrium time" and it will be less if the current speed is higher (Baas, 1999). Once the system develops a bedform equilibrium, if a changes of any control factor, such as current speed, flow depth or grain size, must lead to a morphology change of existing dunes to re-adapt to the new conditions, developing a new bedform equilibrium (Cuadrado *et al.*, 2003). But the bedform response to flow variations is not lineal. Small bedforms experience morphology changes in short times to re-equilibrate with the acting flow. Larger bedforms, such as dunes, experience a longer delay between changes and the moment of equilibrium. If the duration of real tidal currents is less than the equilibrium time, the system can only act on the crest of previous dunes but not on other parameters such as the wavelength. This process induces the co-existence of bedforms formed at different tidal cycles, which show different morphologies and dimensions. According to Dalrymple and Rhodes (1995), it is common that medium and large dunes present an asymmetry that indicates a general migration oriented in the direction of net sediment transport, whereas minor forms are oriented by acting flow. This bedform distribution was also observed in other mesotidal estuarine channels like Bahía Blanca, Argentina (*e.g.* Aliotta and Perillo, 1987; Gómez *et al.*, 2010) or inlets like Grådyb channel, Denmark (Bartholomä *et al.*, 2004), but in these cases the bedforms were developed in deeper areas. In the Piedras River, larger dunes display a persistent ebb-direction because flood, as a subordinate current, cannot transport enough sediment to reverse dune profile. The only place where flood-oriented dunes were observed was the marginal flood channel, where the dominant flow is inverse. At the same time, in the frontal area of intertidal ebb-tidal delta levees, swash bars migrate landwards to be reworked by tidal current when they reach the inlet. This is the normal behaviour described by Oertel (1972) and Sha (1990) in levees of mixed energy ebb-tidal deltas which are considered swash platforms. Unfortunately, side-scan sonar records cannot accurately identify a position of dune crests that allows measurements of migration rates in order to quantify sand volume transported by tide currents and waves.

CONCLUSIONS

Side-scan sonar recordings show different bedform fields in the Piedras River mouth, such as sand patches, dunes and ripples, which have been observed and measured

in different conditions of tidal ranges. Deeper channel areas are connected with the ebb tidal delta, which are areas of sediment bypass. The presence of large bedforms and great mobility indicate a high-energy transport. Sediment transport is reversed during ebb and flood. In ebb direction dominant tidal channels, net sand transport is seawards, where waves and tides act in crosswise directions. Both forces cause an eastward migration of the barrier-island system.

Large bedforms migrate when current velocity reaches the threshold values for movement, which is indicative of extreme conditions. Ebb dunes are most abundant and bigger than flood bedforms. Large dunes originated under ebb conditions retain their preferred asymmetric orientation that cannot be reversed and they migrate in the opposite direction. Small bedforms, such as ripples, are able to reverse their asymmetry and migration direction, and are always active according to currents. The study area shows a low to medium flow regime, corresponding to a moderate hydrodynamism level, enough to transport sand along tidal channels. On the other hand, a low rate of terrigenous supply and the presence of submarine rocky outcrops indicate a depositional regime controlled by accommodation. These depositional conditions, apparently contradictory, partly explain the stability and permanence of the barrier island system developed at the Piedras River mouth. While a depositional balance is maintained in barrier back tidal currents, compensating erosional-depositional effects, in open zones waves act as an energetic barrier that prevents sand from being transported outside of the littoral system, except during very high-energy conditions, such as when major storms or tsunami waves affect the coast (Morales *et al.*, 2008).

ACKNOWLEDGMENTS

This study has been done in the setting of the Group RNM-276 funded by the Research Plan from the University of Huelva, the Andalousian Plan for Investigation, Development and Innovation (PAIDI), the Project CGL2010-16878 from the National Plan of I+D+i (Dirección General de Investigación, Ministerio de Ciencia, Innovación y Competividad, Spain/ FEDER) and I+D agreement with the Andalousian Agency of Harbours (APPA).

REFERENCES

Aliotta, S., Perillo, G.M.E., 1987. A sand wave field in the entrance to the Bahía Blanca Estuary, Argentina. Marine Geology, 76, 1-14.

Anthony, D., Leth, J.O., 2002. Large-scale bedforms, sediment distribution and sand mobility in the eastern North Sea off the Danish west coast. Marine Geology, 182, 247-263.

Ashley, G.M., 1990. Classification of large scale subaqueous bedforms: a new look at an old problem. Journal of Sedimentary Petrology, 60, 160-172.

Baas, J.H., 1999. An empirical model for the development and equilibrium morphology of current ripples in fine sand. Sedimentology, 46, 123-138.

Bartholdy, J., Bartholoma, A., Flemming, B.W., 2002. Grain-size control of large compound flow-transverse bedforms in a tidal inlet of the Danish Wadden Sea. Marine Geology, 188, 391-413.

Bartholomä, A., Ernstsen, V.B., Flemming, B.W., Bartholdy, J., 2004. Bedform dynamics and net sediment transport paths over a flood-ebb tidal cycle in the Grådyb channel (Denmark), determined by high-resolution multibeam echosounding. Danish Journal of Geography, 104(1), 45-55.

Borrego, J., Morales, J.A., Pendón, J.G., 1993. Holocene filling of an estuarine lagoon along the mesotidal coast of Huelva: the Piedras River mouth, Southwestern Spain. Journal of Coastal Research, 9, 242-254.

Carling, P.A., Golz, E., Orr, H.G., Radecki-Pawlik, A., 2000. The morphodynamics of fluvial sand dunes in the River Rhine, near Mainz, Germany. Part I. Sedimentology and morphology. Sedimentology, 47, 227-252.

Costa, S., Gutiérrez-Mas, J.M., Morales, J.A., 2009. Establecimiento del régimen de flujo en el estuario del Guadalquivir, mediante el análisis de formas de fondo con sonda multihaz. Revista de la Sociedad Geológica de España, 22(1-2), 23-42.

Cuadrado, D.G., Gómez, E.A., Ginsberg, S.S., 2003. Large transverse bedforms in a mesotidal estuary. Revista Asociación Argentina de Sedimentología, 10(2), 163-172.

Dabrio, C., 1982. Sedimentary structures generated on the foreshore by migrating ridge and runnel systems on microtidal and mesotidal coast on S Spain. Sedimentary Geology, 32, 141-151.

Dalrymple, R.W., Rhodes, R.N., 1995. Estuarine dunes and bars. In: Perillo, G.M.E. (ed.). Geomorphology and Sedimentology of Estuaries. Developments in Sedimentology, Amsterdam, Elsevier, 53, 359-422.

Davis Jr., R.A., Kuhn, B.J., 1985. Origin and development of Anclote Key, west-peninsular Florida. Marine Geology, 63, 153-171.

Delgado, I., Morales, J.A., Gutiérrez-Mas, J.M., 2005. Dinámica de formas de fondo en la desembocadura del estuario del Río Piedras (Huelva). Geogaceta, 38, 143-146.

Delgado, I., Morales, J.A., Gutiérrez-Mas, J.M., 2007. Movilidad de las formas de fondo en la desembocadura del estuario del Río Piedras (Huelva) durante las mareas vivas. Geogaceta, 43, 87-90.

Duck, R.W., Rowan, J.S., Jenkins, P.A., Youngs, I., 2001. A multi-method study of bedload provenance and transport pathways in an estuarine channel. Physics and Chemistry of the Earth, Part B: Hydrology. Oceans and Atmosphere, 26, 747-752.

Fenster, M.S., Fitzgerald, D.M., Bohlen, W.F., Lewis, R.S., Baldwin, C.T., 1990. Stability of giant sand waves in Eastern Long Island Sound, U.S.A. Marine Geology, 91, 207-225.

Fitzgerald, D.M., 1988. Shoreline erosional–depositional processes associated with tidal inlets. In: Aubrey, D.G., Weishar, L. (eds.). Hydrodynamics and Sediment Dynamics of Tidal Inlets. New York, Springer-Verlag, 269-283.

Fitzgerald, D.M., Buynevich, I.V., Davis Jr.R.A., Fenster, M.S., 2002. New England tidal inlets with special reference to riverine-associated inlet. Geomorphology, 48, 179-208.

Garnaud, S., Lesueur, P., Clet, M., Lesourd, S., Garlan, T., Lafite, R., Brun-Cottan, J.C., 2003. Holocene to modern fine-grained sedimentation on a macrotidal shoreface-to-inner-shelf setting (eastern Bay of the Seine, France). Marine Geology, 202, 33-54.

Gómez, E.A., Cuadrado, D.G., Pierini, J.O., 2010. Sand transport on an estuarine submarine dune field. Geomorphology, 121, 257-265.

Grant, W.D., Madsen, O.S., 1982. Mobile bed roughness an unsteady oscillatory flow. Journal Geophysical Resources, 87, 469-481.

Gutiérrez Mas, J.M., Juan, C., Morales, J.A., 2009a. Evidence of high-energy events in shelly layers interbedded in coastal Holocene sands in Cadiz Bay (south-west Spain). Earth Surface Processes and Landforms, 34, 810-823.

Gutiérrez-Mas, J.M., López-Arroyo, J., Morales, J.A., 2009b. Recent marine lithofacies in the Cadiz Bay (SW Spain). Sequences, Processes and control factors. Sedimentary Geology, 218, 31-47.

Harbor, D.J., 1998. Dynamics of bedforms in the lower Mississippi River. Journal of Sedimentary Research, 68, 750-762.

Harms, J.C., Southard, J.B., Spearing, D.R., Walker, R.G., 1975. Depositional environments from primary sedimentary structures and stratification sequences. Dallas, SEPM Short Course 2, 161pp.

Harris, P.T., Collins, M.B., 1984. Bedform distributions and sediment transport paths in the Bristol Channel and Severn Estuary, U.K. Marine Geology, 62, 153-166.

Hayes, M.O., 1980. General morphology and sediment patterns in tidal inlets. Sedimentary Geology, 26, 139-156.

Hicks, D.M., Hume, T.M., 1996. Morphology and size of ebb-tidal deltas at natural inlets on open-sea and pocket bay coasts, North Island, New Zealand. Journal of Coastal Research, 12, 47-63.

Hicks, M.D., Hume, T.M., Swales, A., Green, M.O., 1999. Magnitudes, spatial extent, time scales and causes of shoreline changes adjacent to an ebb–tidal delta, Katikati Inlet, New Zealand. Journal of Coastal Research, 15, 220-240.

Imperato, D.P., Sexton, W.J., Hayes, M.O., 1988. Stratigraphy and sediment charasteristics of a mesotidal ebb-tidal delta, North Edisto Inlet, South Carolina. Journal of Sedimentary Petrology, 58, 950-958.

Knebel, H.J., Rendigs, R.R., Oldale, R.N., Bothner, M.H., 1992. Sedimentary framework of Boston Harbor, Massachusetts. In: Fletcher III, C.H., Wehmiller, J.F. (eds.). Quaternary Coasts of the United States: Marine and Lacustrine Systems. SEPM, 48(Special Publication), 48, 35-43.

Kuijpers, A., Werner, F., Rumohr, J., 1993. Sandwaves and other large-scale bedforms as indicators of non-tidal surge currents in the Skagerrak on Northern Denmark. Marine Geology, 111, 209-221.

Langhorne, D.N., 1973. A sandwave field in the outer Thames estuary, Great Britain. Marine Geology, 14, 129-143.

Lobo, F.J., Plaza, F., González, R., Dias, J.M.A., Kapsimalis, V., Mendes, I., Díaz del Río, V., 2004. Estimations of bedload sediment transport in the Guadiana Estuary (SW Iberian Peninsula) during low river discharge periods. Journal of Coastal Research, 41, 12-26.

McKinney, T.F., Stubblefield, W.L., Swift, D.J.P., 1974. Large-scale current lineations on the central New Jersey shelf: Investigations by side-scan sonar. Marine Geology, 17, 79-102.

Morales, J.A., 1997. Evolution and facies architecture of the mesotidal Guadiana River delta (SW Spain, Portugal). Marine Geology, 138, 127-148.

Morales, J.A.; Borrego, J., Jiménez, I., Monterde, J.R., Gil, N., 2001. Morphostratigraphy of an ebb-tidal delta system associated with a large spit in the Piedras Estuary mouth (Huelva Coast, Southwestern Spain). Marine Geology, 172, 225-241.

Morales, J.A., Delgado, I., Gutiérrez-Mas, J.M., 2006. Sedimentary characterization of bed types along the Guadiana Estuary (SW Europe) before the construction of the Alqueva dam. Estuarine, Coastal and Shelf Science, 70, 117-131.

Morales, J.A., Borrego, J., San Miguel, E.G., López-González, N., Carro, B.M., 2008. Sedimentary record of recent tsunamis in the Huelva Estuary (Southwest Spain). Quaternary Science Reviews, 27, 734-746.

Morales, J.A., Gutiérrez-Mas, J.M., Borrego, J., Rodríguez-Ramírez, A., 2011. Sedimentary Characteristics of the Holocene Tsunamigenic Deposits in the Coastal Systems of the Cadiz Gulf (Spain). In: Mörner, N.A. (ed.). The Tsunami Threat-Research and Technology. Rijeka, InTech, 237-258.

Nichol, S.L., Boyd, R., 1993. Morphostratigraphy and facies architecture of sandy barriers along the Eastern Shore of Nova Scotia. Marine Geology, 114, 59-80.

Oertel, G.F., 1972. Sediment transport in estuarine entrance shoals and the formation of swash platforms. Journal of Sedimentary Petrology, 42, 857-863.

Ojeda, J., Vallejo, I., 1995. La Flecha de El Rompido: análisis morfométrico y modelos de evolución durante el periodo 1943-1991. Revista de la Sociedad Geológica de España, 8, 229-238.

Rubin, D.M., 1987. Cross-bedding Bedforms and Paleocurrents. Society of Economic Paleontologist and Mineralogist. Concepts in Sedimentology, 1, 183pp.

Salsman, G.G., Tolbert, W.H., Villars, R.G., 1966. Sand ridge migration in St. Andrews Bay, Florida. Marine Geology, 4, 11-19.

Sha, L.P., 1990. Sedimentological studies of the ebb-tidal deltas along the West Frisian Islands, the Netherlands. Geologica Ultraiectina, 64, 160pp.

Sherwood, C.R., Creager, J.S., 1990. Sedimentary geology of the Columbia River Estuary. Progress in Oceanography, 25, 15-79.

Southard, J.B., Boguchwal, L.A., 1990. Bed configuration in steady unidirectional water flows: part 2. Synthesis of flume data. Journal of Sedimentary Petrology, 60, 658-679.

Van Heteren, S., Oost, A.P., van der Spek, A.J.F., Elias, E.P.L., 2006. Island-terminus evolution related to changing ebb-tidal-delta configuration: Texel, The Netherlands. Marine Geology, 235, 19-30.

Van Lancker, V., Lanckneus, J., Moerkerke, G., Hearn, S., Hoekstra, P., Levoy, F., 2004. Coastal and nearshore morphology, bedforms and sediment transport pathways at Teignmouth (UK). Continental Shelf Research, 24, 1171-1202.

Van Rijn, L.C., 1993. Principles of sediments transport in rivers, estuaries and coastal seas. Deft, Aqua Publications, 110pp.

Woodruff, J.D., Geyer, W.R., Sommerfield, C.K., Driscoll, N.W., 2001. Seasonal variation of sediment deposition in the Hudson River estuary. Marine Geology, 179, 105-119.

Wright, L.D., Prior, D.B., Hobbs, C.H., Byrne, R.J., Boon, J.D., Schaffner, L.C., Green, M.O., 1987. Spatial variability of bottom types in the lower Chesapeake Bay and adjoining estuaries and inner shelf. Estuarine, Coastal and Shelf Science, 24, 765-784.

Wu, J., Wang, Y., Cheng, H., 2009. Bedforms and bed material transport pathways in the Changjiang (Yangtze) Estuary. Geomorphology, 104, 175-184.

Manuscript received November 2013;
revision accepted February 2015;
published Online June 2015.